

Aus der
Klinik für Kleintiere
der Veterinärmedizinischen Fakultät der Universität Leipzig

Bestimmung der radio-ulnaren Inkongruenz bei Hunden mit Ellbogen-gelenksdysplasie anhand von 3D-Rekonstruktionen

Inaugural-Dissertation
zur Erlangung des Grades eines
Doctor medicinae veterinariae (Dr. med. vet.)
durch die Veterinärmedizinische Fakultät
der Universität Leipzig

eingereicht von
Hamdi Mohammed Eljack
aus Bahri (Sudan)

Leipzig, 2015

Mit der Genehmigung der Veterinärmedizinischen Fakultät der Universität Leipzig

Dekan: Prof. Dr. Manfred Coenen

Betreuer: Prof. Dr. Peter Böttcher

Gutachter: Prof. Dr. Peter Böttcher, Klinik für Kleintiere,
Veterinärmedizinische Fakultät, Universität Leipzig
Prof. Dr. Andrea Meyer-Lindenberg, Zentrum für Klinische
Tiermedizin, Chirurgische u. Gynäkologische Kleintierklinik,
Ludwig Maximilians-Universität München

Tag der Verteidigung: 03.11.2015

Meinen Eltern, Meiner Frau und meiner Tochter

Inhaltsverzeichnis

1	EINLEITUNG	1
2	PUBLIKATIONEN	3
2.1	Sensitivity and specificity of 3D models of the radioulnar joint cup in combination with a sphere fitted to the ulnar trochlear notch for estimation of radioulnar incongruence in vitro	3
2.2	Relationship between axial radio-ulnar incongruence with cartilage damage in dogs with medial coronoid disease	16
3	DISKUSSION	32
4	ZUSAMMENFASSUNG	36
5	SUMMARY	38
6	LITERATURVERZEICHNIS	40

Abkürzungsverzeichnis

aRUI	axiale radio-ulnare Inkongruenz
BW	Body Weight
CT	Computertomographie
DOR	Diagnostisches Quotenverhältnis
ED	Ellbogengelenksdysplasie
ICC	Intraklassen-Korrelationskoeffizient
FPC	Fragmentierter <i>Processus coronoideus medialis ulnae</i>
IPA	Isolierter <i>Processus anconaeus</i>
MCD	Medial Coronoid Disease
MPC	<i>Processus coronoideus medialis ulnae</i>
OCD	Osteochondrosis dissecans
RUI	Radio-ulnare Inkongruenz
SD	Standardabweichung
DPUO	Dynamische Proximale Ulna Osteotomie
3D	Dreidimensional

1 Einleitung

Das Ellbogengelenk des Hundes ist ein komplexes Gelenk, welches sich aus Humerus, Radius und Ulna zusammensetzt. Die häufigsten klinischen Ausprägungen der Ellbogengelenksdysplasie (ED) bei jungen schnellwüchsigen Rassen sind der isolierte Processus anconaeus (IPA), der fragmentierte Processus coronoideus medialis ulnae (FPC) und die Osteochondrosis dissecans (OCD) (WIND 1986, KIRBERGER und FOURIE 1998, MORGAN et al. 1999). Die Ellbogengelenksinkongruenz ist eine weitere Form der ED (WIND 1986, KIRBERGER und FOURIE 1998, BRUNNBERG et al. 1999, COLLINS et al. 2001, GIELEN et al. 2001, PRESTON et al. 2001, MASON et al. 2002), welche zu degenerativen Gelenkerkrankungen und Lahmheiten führen kann (WIND 1986, PRESTON et al. 2001, MASON et al. 2002, SJÖSTRÖM et al. 1995, MORGAN et al. 1999).

Die radio-ulnare Inkongruenz (RUI), hauptsächlich in Form der positiven RUI mit einem kürzeren Radius in Relation zur Ulna, wurde als eine mögliche Ursache der mechanischen Überlastung im medialen Gelenkkompartiment beschrieben (SA-MOY et al. 2006, GEMMILL und CLEMENTS 2007), wodurch es zum FPC und im fortgeschrittenen Stadium dem medialen Kompartiment-Syndrom kommen kann. Letzteres ist durch Abrieb des Gelenkknorpels am medialen Processus coronoideus und an der Trochlea humeri gekennzeichnet (DANIELSON et al. 2006, KRAMER et al. 2006). Das "Traditional Linear Model" der RUI, mit einer relativen radialen Verkürzung erklärt allerdings die Koexistenz von FPC und IPA im selben Gelenk nicht (MEYER-LINDENBERG et al. 2006), weil der IPA im Verdacht steht, sich auf Grund einer relativen ulnaren Verkürzung (negativer RUI) gegenüber dem Radius zu entwickeln (SJÖSTRÖM et al. 1995).

Das "Angular-Vector Model" ist eine Erweiterung des "Traditional Linear Model", in dem sowohl eine kurze Ulna (negative RUI) und ein kurzer Radius (positive RUI) zur mechanischen Überlastung des medialen Kompartiments, insbesondere des Processus coronoideus medialis ulnae führen (LOZIER 2006). Bisher gibt es keine Belege, dass eine negative RUI zu entsprechenden mechanischen Schäden im medialen Gelenkabschnitt führt, und es ist nichts über die Inzidenz einer negativen RUI im Zusammenhang mit Koronoiderkrankungen bekannt.

In der Literatur sind bisher zahlreiche radiologische Techniken zur Diagnose einer Ellbogengelenksinkongruenz beschrieben (BLOND et al. 2005, SAMOY et al.

2006). Allerdings erfolgt die Beurteilung oftmals subjektiv und die Genauigkeit bei der Bestimmung kleiner Stufen (≤ 2 mm) ist ungenügend (MASON et al. 2002). In der klinischen Praxis hat sich die Computertomographie (CT) als Standard für die Messung der RUI etabliert, wobei der CT eine geringe Spezifität attestiert wird (WAGNER et al. 2007). Zudem konnte zwischen der in reformatierten CT-Bildern gemessenen RUI und dem Ausmaß an Knorpelschäden im medialen Kompartiment kein eindeutiger Zusammenhang festgestellt werden. Ein Umstand der in Folge von Messungenauigkeiten bei der RUI-Bestimmung zu erklären wäre, oder mit dem Fehlen eines biologischen Zusammenhangs zwischen RUI und Gelenkpathologie (KRAMER et al. 2006). Das im Moment sensitivste und spezifischste Diagnostikum ist die Arthroskopie (WAGNER et al. 2007, WERNER et al. 2009). Diese ist aber invasiv, stark von der Erfahrung des Operateurs abhängig und bisher nur in vitro evaluiert. Klinsche Studien zur arthroskopischen Bestimmung der RUI fehlen in der Literatur.

Die dreidimensionale (3D) Darstellung der radioulnaren Gelenkpfanne basierend auf transversalen CT-Bildern des Ellenbogens, ermöglicht die ungehinderte visuelle Beurteilung der radio-ulnaren Konformation, sowie die semiquantitative Abschätzung der vorliegenden positiven wie auch negativen Stufe (BÖTTCHER et al. 2009). Allerdings ist die Technik mit einer Sensitivität von 0,86 und einer Spezifität von 0,77 für die klinische Anwendung immer noch zu ungenau, da eine hohe Zahl falsch positiver Diagnosen zu erwarten ist.

Ziel der vorliegenden Studie war es, die 3D-Technik zur Bestimmung einer RUI in ihrer Genauigkeit zu verbessern und mit Hilfe der verbesserten Technik die Beziehung zwischen der Form und Ausprägung einer vorliegenden RUI und dem Grad an artikulärem Schaden im medialen Kompartiment zu untersuchen.

2 Publikationen

2.1 Sensitivity and specificity of 3D models of the radioulnar joint cup in combination with a sphere fitted to the ulnar trochlear notch for estimation of radioulnar incongruence in vitro

Hamdi Eljack , BVM, Hinnerk Werner, DVM, Dr. med. vet., and Peter Böttcher , DVM, Prof. Dr. med. vet., Diplomate ECVS

Veterinary Surgery 2013; 42(4): 365-370.

Objective: To determine the sensitivity and specificity of estimation of radioulnar incongruence (RUI) by use of 3-dimensional (3D) image renderings in combination with a sphere fitted to the ulnar trochlear notch.

Study Design: In vitro study.

Sample Population: Right forelimbs ($n = 8$) of canine cadavers weighing >20 kg

Methods: CT based 3D models ($n = 63$) of the radioulnar joint cup with different states of RUI were used. A sphere was fitted to the trochlear notch of each of the models and 2 independent observers estimated RUI based on the relation of the sphere and the radial joint surface blinded to the true state of RUI at 1 mm precisely (-2 mm to + 2 mm).

Results: Mean sensitivity and specificity for detecting any form of incongruent joint was 0.94 and 0.89, respectively. Evaluating a positive step (short radius) versus a congruent joint resulted in a mean sensitivity and specificity of 0.89 and 0.96, respectively. A negative RUI (short ulna) was diagnosed with a mean sensitivity and specificity of 1.00 and 0.92, respectively. Intra-class-correlation coefficient for inter-observer agreement was 0.99.

Conclusions: Fitting a sphere to the ulnar trochlea notch significantly improves diagnostic accuracy of 3D models of the radioulnar joint cup when diagnosing RUI.

Introduction

The canine elbow joint is a complex joint formed by the distal aspect of the humerus and the proximal aspects of the radius and ulna. Elbow incongruence refers to a mal-alignment of these 3 bones within the joint,¹⁻⁸ representing 1 type of elbow dysplasia (ED), resulting in degenerative joint disease and lameness.^{1,7-10} The most recognized clinical presentations of ED are ununited anconeal process (UAP), fragmented medial coronoid process (FCP) and osteochondrosis dissecans (OCD) of the medial part of the humeral condyle, occurring most frequently in juvenile, large breed dogs.^{1,2,10}

Radio-ulnar incongruence (RUI) is a multifactorial process,¹¹⁻¹⁵ in which a step formation within the radio-ulnar joint cup may lead to mechanical overload of the medial compartment of the joint,^{14,15} potentially inducing fragmentation of the medial coronoid process and in advanced stages medial compartment syndrome, which is characterized by abrasion of joint cartilage at the medial coronoid process and the humeral trochlea.^{13,16} Depending whether the step formation is the result of an ulnar joint surface being more proximal than the radial head or the reverse, were the radial head surmounts the ulnar joint surface, 2 hypotheses, explaining the mechanism of mechanical overload and subsequent FCP formation or medial compartment syndrome, have been proposed. The "Traditional Linear Model" is characterized by a relative radial shortening or ulnar lengthening, both resulting in positive RUI,¹ where the positive step formation at the level of the radio-ulnar joint surface results in focal pressure accumulation at the medial coronoid process and opposing humeral trochlea. This model however fails to explain the coexistence of FCP and UAP in the same joint,¹⁷ because UAP is thought to develop because of relative shortening of the ulna (negative RUI) compared to the radius.⁹ The "Angular-Vector Model" is an extension of the "Traditional Linear Model", in which both a short ulna (negative RUI) or short radius (positive RUI) lead to mechanical overloading of the medial compartment particularly the medial coronoid process and the humeral trochlea.¹⁸ The biomechanical concept for the short radius (positive RUI) is identical to the one of the "Traditional Linear Model"; however, with the "Angular-Vector Model" relative overgrowth of the radius (negative RUI; short ulna) is believed to increase intraarticular pressure within the medial joint compartment by pushing against the lateral aspect of the humeral condyle. Because the humeral condyle is in contact with the anconeal

process, any pressure from the radial head will result in a rotatory moment with the anconeal process as pivot point, rotating the medial aspect of the humeral condyle distally, and therefore increasing the pressure at the medial coronoid process.

Several radiographic features to diagnose elbow incongruity have been described,^{12,15} but the 'scoring' of incongruity is still subjective and doesn't allow for precise quantitative measurement of RUI, especially when considering small steps (1 - 2 mm).⁸ In clinical practice, computed tomography (CT) has been accepted as reference standard for the measurement of RUI, but has recently been reported to be of low specificity.¹⁹ Arthroscopic grading of RUI has been proven to be the most accurate modality so far,^{19,20} but it is invasive and operator dependent, limiting its broad application in the diagnosis of RUI. 3D-renderings of the radioulnar joint surface, based on transverse CT images of the elbow, allow for unobstructed inspection of the radioulnar transition and semi-quantitative estimation of both negative and positive RUI.²¹ However, with a reported sensitivity of 0.86 and a specificity of 0.77,²¹ clinical application of this technique would still result in a significant number of false positive and false negative diagnoses. The reason for the limited specificity of the 3D models in the diagnosis of RUI may be based on the fact, that even in perfectly congruent joints a radioulnar step is visible on 3D models of the subchondral joint surface, to some point pretending a true, pathological RUI.

Our purpose is to extend the 3D model technique by fitting a sphere to the trochlear notch of the ulna, resulting in a visual aid for the observer when appreciating the continuity of the radioulnar joint cup and thereby improving the accuracy of RUI estimation.

Materials and Methods

3D Models

3D models of the radioulnar joint cup ($n = 63$) from a previous in vitro study on the sensitivity and specificity of 3D image renderings of the elbow for the diagnosis of RUI were used.²¹ In the original study 64 models had been generated, but since then 1 data set had been corrupted and could not be used in the current study, yielding 63 models available for study. The 3D models were based on cadaveric right thoracic limbs of 8 mature, middle to large breed dogs (weighing >20 kg) with no history of or-

thopedic disease. All 8 elbows joints were free of any detectable joint pathology, based on complete radiographic and CT examination, and gross inspection of the joint at the end of the study.

RUI had been induced using a linear side-bar in the form of a 4-pin type 1 unilateral external skeletal fixator applied to the cranial aspect of the osteotomized radial diaphysis. This allowed for precise shortening as well as lengthening of the radius at 1mm increments from 0 - 2mm, with a correlation coefficient (R-value) of 0.996 ($R^2=0.992$) between the relative movement of the proximal radius with respect to the native unchanged elbow and the presumed proximodistal movement of the radius exerted by the side-bar.²¹ Each time the linear side bar had been lengthened or shortened, a complete transverse CT scan of the elbow joint had been performed simulating sternal recumbency with the elbow joint at an angle of ~135°. Acquisition of CT data had been performed on a multi-slice helical CT-scanner (Philips Brilliance, Philips, Netherlands) with an average in-plane resolution of 0.159 mm (SD = 0.011 mm) and a slice thickness of 1 mm with an overlapping increment of 0.5 mm. Image reconstruction was done using a sharp bone filter (FilterType and ConvolutionKernel D).

In each resulting CT data set, the humerus had been manually segmented and removed from the data using MevisLab (MeVisLab 2.0, MeVis Medical Solutions AG, Bremen, Germany, www.mevislab.de). Finally, 3D surface-reconstructions of the radioulnar joint cup had been calculated using dedicated image analysis software based on the VTK (VTK 3.0, Kitware, Inc., NY, www.vtk.org). Further enhancement as well as inspection of the 3D-models were performed using ParaView (ParaView 3.0, Kitware, Inc; www.paraview.org). All together eight 3D models for each elbow with 4 incongruent (-2, -1, +1, +2mm), 1 congruent (0mm), and 3 randomly chosen repetitions (from -2 over 0 to +2mm) had been generated.²¹ The sixty-three 3D models evaluated in the current study were divided as: 11x -2 mm RUI, 11x -1 mm RUI, 13x congruent joints, 14x +1mm RUI, and 14x +2mm RUI. The corrupted model had had a RUI of -1mm.

Sphere Fitting Technique

After randomization of the available 63 3D radioulnar models using a freely available random list generator (www.random.org), the surface points of the sagittal ridge of the trochlear notch were selected using the paint brush tool within ParaView (Fig 1A). The 3D coordinates of those points were feed to a software script (MATLAB 9.0, The MathWorks, Inc., Natick, MA) that calculates a best fitting sphere (Fig 1B), based on the algorithm by Taubin.²² In the context of this algorithm "best fit" means the sphere minimizes the sum of squared distances from the points to the surface of the sphere. Once an optimal sphere was found it was added to the virtual scene (Fig 1C).

Estimation of RUI

The complete series of 3D models ($n = 63$) with the fitted sphere in place were evaluated in random order, by 2 investigators blinded to the true state of radioulnar conformation. They were free to inspect each 3D model at their own pace by moving, scaling, and rotating the model with the connected sphere on the computer screen. The degree of RUI present was estimated based on the relation of the fitted sphere and the caudal radial joint surface (Fig 2). Congruence is characterized by a continuous contact between the sphere and the anconeal process, the distal edge of the trochlea notch and the caudal radial head. Positive RUI is characterized by a clear space between the sphere and the radial head, while negative RUI is characterized by collision of the sphere and the radial head. By up- and down-scaling of the sphere's radius until the sphere barely touched the caudal radial joint surface estimation of the degree of RUI was performed at 1 mm precision from -2 to +2 mm.

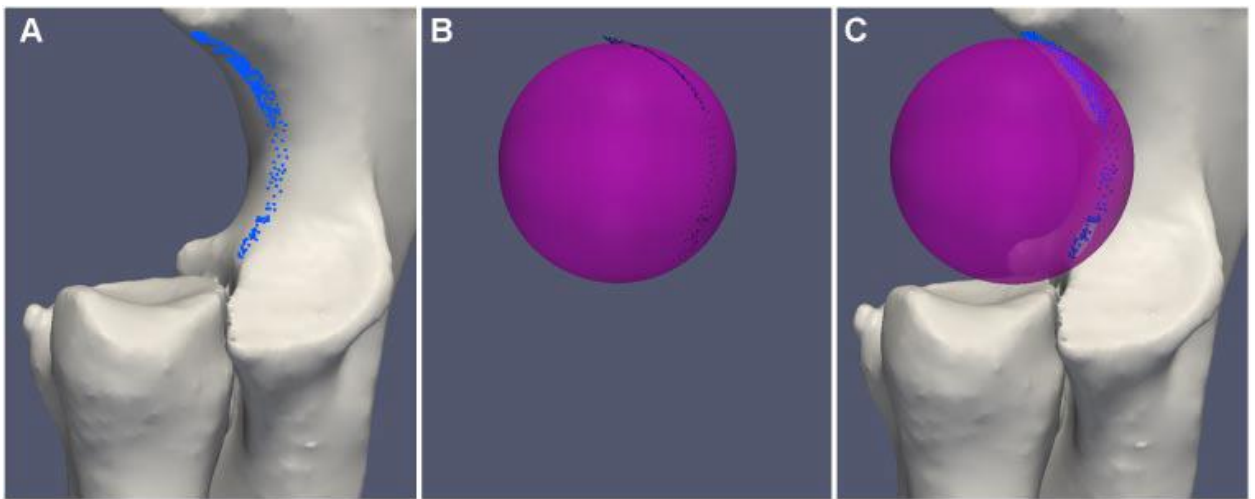


Fig. 1: Process of constructing and fitting a sphere to the trochlear notch. A) Selection of surface points along the sagittal ridge of the trochlear notch using a paintbrush type tool within ParaView. B) Extraction of the point cloud and transfer of the 3D-coordinates of the selected points to a MATLAB script, calculating the best fitting sphere, where the majority of the points lies on the surface of the calculated sphere. C) Combination of the generated sphere and the radial and ulnar models.

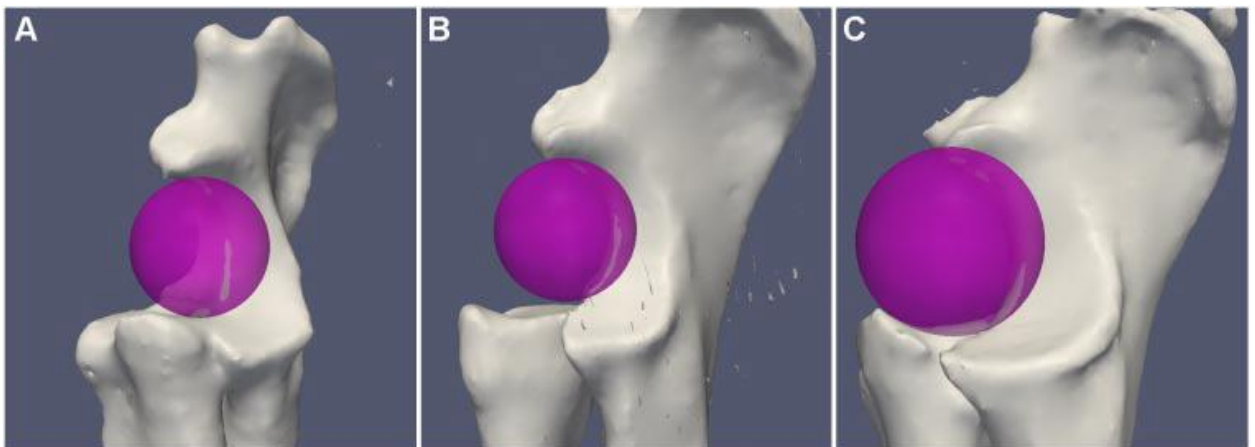


Fig. 2: Typical appearance of a congruent and two incongruent models with the corresponding sphere fitted to the trochlear notch. A) Congruence is characterized by a continuous contact between the sphere and the anconeal process, the distal edge of the trochlea notch and the caudal radial head. B) Positive RUI is characterized by a clear space between the sphere and the radial head. C) Negative RUI is characterized by collision of the sphere and the radial head.

Data Analysis

Sensitivity and specificity were calculated based on cross-table calculation for each investigator separately. The overall sensitivity and specificity were expressed as the mean of the 2 investigators. Sensitivity and specificity in relation to 3 different definitions of RUI were calculated: 1) estimation of an incongruent versus a congruent joint, summarizing all states of RUI different from a congruent joint; 2) all positive RUIs versus the congruent joint; and 3) all negative RUIs versus the congruent joint. Because the study design used 2 possible states of incongruence, underestimation of specificity would be inevitable when applying the traditional definition of a congruent joint as “the unmodified elbow”. Therefore in scenarios 2 and 3, false positive scores opposed to the investigated type of RUI (positive or negative) were counted as true negative. Estimation of the overall diagnostic test performance of the sphere fitting technique was done using the diagnostic odds ratio (DOR).²³

The DOR is a single indicator of test performance in contrast to paired indicators such as sensitivity and specificity. The following formula was used to calculate DOR: $(\text{mean sensitivity} / (1 - \text{mean sensitivity})) / ((1 - \text{mean specificity}) / \text{mean specificity})$. The value of DOR ranges from 0 to ∞ , with higher values indicating better discriminatory test performance. Any test with a DOR of 1 does not discriminate between elbows with incongruence and those without it. Values < 1 point to improper test interpretation (more negative tests among the incongruent joint).²³ Finally agreement of the individual observer's scoring with the true state of RUI was expressed by intra-class correlation coefficient (ICC) analysis as well as Cronbach's α . The intra-class correlation coefficient (ICC) using an absolute agreement definition was used to quantify inter-observer variability. All calculations were carried out using software (MedCalc, v9.4.2.0, MedCalc Software, Mariakerke, Belgium).

Results

The ratings of the 63 models of the 2 investigators separately (Table 1) reveals overall very high accuracy for both observers. This is reflected by a mean ICC for absolute agreement between the observer's individual score and the true state of RUI (at 1 mm precisely) of 0.97 (95%CI: 0.93, 0.98), with a mean Cronbach's α of 0.98 (range, 0.98 – 0.98). Mean sensitivity for detecting any form of incongruent joint was

0.94 (range, 0.94 - 0.94), mean specificity was 0.89 (range, 0.85 – 0.92), and DOR was 126.77 (Table 2).

Evaluating a positive step versus a congruent joint simulating a shortened radius resulted in a mean sensitivity of 0.89 (range, 0.89 – 0.89), a mean specificity of 0.96 (range, 0.92 – 1.00), and a DOR of 194.18. The shortened ulna reflecting a negative RUI was detected with a mean sensitivity of 1.00 (range, 1.00 – 1.00), a mean specificity of 0.92 (range, 0.92 – 0.92), and a DOR of >1138.50. Sensitivity had been reduced to 0.99 for the calculation of DOR, because division by zero with sensitivity of 1.00 is not allowed. ICC for inter-observer reliability was 0.99 (95% CI: 0.98, 0.99) with a Cronbach's α of 0.99.

Table 1: Cross-table summarizing the results of the 2 investigators for the 63 models of RUI investigated.

		3D-Evaluation					True incidence
		-2 mm	-1 mm	0 mm	+1 mm	+2 mm	
Gold Standard	-2 mm	11 - 10	/ - 1				11
	-1 mm	2 - 1	9 - 10				11
	0 mm		1 - 1	12 - 11	/ - 1		13
	+1 mm			3 - 3	10 - 10	1 - 1	14
	+2 mm				2 - 2	12 - 12	14
Estimated incidence		12 - 11	10 - 11	15 - 14	12 - 13	13 - 13	

The results for the 2 investigators are listed separated by a hyphen: investigator 1-investigator 2. The row on the right summarizes the true incidence of each state of RUI within the 63 models investigated. The lower line summarizes the number of estimations of each investigator for the 5 possible states of RUI.

Table 2. Mean sensitivity and specificity together with the individual values of the two observers in parenthesis. Diagnostic odds ratio (DOR) is provided as a measure of overall diagnostic test performance.

	Sensitivity	Specificity	DOR
Congruent vs. incongruent	0.94 (0.94 – 0.94)	0.89 (0.85-0.92)	126.76
Congruent vs. positive RUI	0.89 (0.89 – 0.89)	0.96 (0.92-1.00)	194.18
Congruent vs. negative RUI	1.00 (1.00 – 1.00)	0.92 (0.92 - 0.92)	>1138.50*

* Sensitivity was reduced to 0.99 for the calculation of DOR, because division by zero with sensitivity of 1.00 is not allowed.

DISCUSSION

Studies focusing on both positive as well as negative RUI are rare,^{20,21} making comparison of our findings to other reports^{8,12,19,24} that graded positive RUI only, difficult. Nevertheless, with the exception of arthroscopy, the sphere fitting technique appears to outperform all other diagnostic protocols so far. Therefore, our study aim, which was the improvement of diagnostic accuracy of the 3D rendering technique was attained, as sensitivity, when adding the sphere for visual aid improved from 0.86 to 0.94, but more importantly specificity, which was unacceptable low with the 3D renderings only, dramatically improved from 0.77 to 0.89 by adding the sphere.²¹ Even interobserver reliability was improved from 0.87 to 0.99 with the sphere fitting technique, which further strengthens its value as a clinical tool in dysplastic elbow joints.

The sphere fitting technique relies on the assumption, that in congruent elbows, the circular geometry of the sagittal ridge of the ulnar trochlea notch perfectly matches the surface of the caudal aspect of the radial head. This is a constant feature observed in 3D models with no RUI (Fig 2A), but may have to be affirmed with a larger number of congruent joints, in a separate study. Incongruence on the other hand, would only be detected as such when using the sphere fitting technique, if the radioulnar step is present at the ulnar incisure, where diagnosis of RUI is reportedly the most accurate.¹⁹ Estimation of RUI at the apex or the mid-body of the medial coro-

noid process,¹⁹ is not possible, limiting the sphere fitting technique to the detection of RUI at the ulnar incisure only.

Being based on the geometry of the ulnar trochlear notch, the sphere fitting technique might be negatively influenced by a dysplastic trochlea notch, the latter being described as one possible form of elbow dysplasia.¹ With a trochlear notch being too small for the humeral condyle to fit,¹ the calculated sphere would be significantly smaller because of the trochlear notch dysplasia, than normally in a joint without RUI, potentially altering the relation of the sphere to the caudal aspect of the radial head, in the way that a positive RUI might be falsely diagnosed. If this scenario would be a serious limitation when using the sphere fitting technique in clinical cases cannot be answered, as we did not have elbow joints with ulnar trochlear notch dysplasia available for testing.

When using 3D renderings based on CT data there are some aspects that might be considered significant limitations when attempting to use the technique on clinical cases.²¹ First of all, CT based measurement of RUI only considers RUI at the level of the subchondral bone, regardless whether multiplanar reconstructions or 3D image renderings are used. This is why one cannot exclude that RUI at the subchondral bone level might be equalized by varying thickness of the overlying radial and ulnar joint cartilage, resulting in a congruent joint despite subchondral RUI. Vice versa, a true RUI at the level of the joint surface might not be visible at the level of the subchondral bone. Another limitation when using CT based measurements are potential positioning artifacts, during CT scanning.²⁵ On the other hand, the degree of extension and rotation of the elbow influence the appearance of the radioulnar transition on arthroscopy,¹⁹ and variation in positioning during plain radiography,¹² significantly affects overall diagnostic performance, too. This is why, probably for any modality, standardized positioning of the limb during data acquisition is mandatory, to reduce positioning artifacts to a minimum. Nevertheless, with the sphere fitting technique positioning artifacts during CT scanning may be expected to be of low relevance, because the technique allows for consistent identification of anatomic landmarks.²⁵ The identification of the points necessary to construct the “best fit” sphere is intuitive and much more reliable on 3D models than on multiplanar reconstructed CT images.

The complexity of the image processing steps to get a high quality 3D rendering of the radioulnar joint cup in combination with a fitted sphere is probably the most im-

portant limitation of the proposed technique, especially when thinking of broad clinical application. Already the creation of the 3D model of the radioulnar joint cup takes about 30 minutes,²¹ because manual slice by slice segmentation of the humerus and subsequent deletion from the data set has to be performed to provide an unobstructed view at the radioulnar joint cup. The manual selection of the surface points along the sagittal ridge of the trochlear notch, transfer of the point coordinates for calculation of the sphere and finally the addition of the sphere to the virtual scene, further increase the time and work to get to a point where the clinician would be able to make a diagnosis. Both processing steps, segmentation and fitting of the sphere, have to be automated to support broad application in the future and the complete imaging pipeline will have to be realized within one program only, making it much more user friendly. Established algorithms for unsupervised delineation of bony contours on CT data fail in the canine elbow joint, because the joint space is so small in some regions that partial volume artifacts join the 3 bones to one interconnected model. 3D third-order sub-pixel edge-driven level-set segmentation has successfully been implemented solving this problem, but the code is in development stage and therefore still not available for public use.

Summarily, adding a fitted sphere to 3D renderings of the radioulnar joint cup improves diagnostic accuracy to a point, where the technique can be considered safe and highly accurate for clinical application. Except arthroscopy, all other imaging protocols to diagnose RUI have much lower diagnostic odds ratios, especially when dealing with small (≤ 2 mm) RUI. Nevertheless, being an in vitro study on sound elbow joints it warrants further evaluation of the proposed methodology in dogs with elbow dysplasia to better ascertain its clinical importance.

Bibliography

1. Wind AP: Elbow incongruity and developmental elbow diseases in the dog: Part I. J Am Anim Hosp Assoc 1986;22: 712–724
2. Kirberger RM, Fourie SL: Elbow dysplasia in the dog: pathophysiology, diagnosis and control. J Sth Afr Vet Assoc 1998;69:43-54
3. Brunnberg L, Viehmann B, Waibl H: Computergestützte Auswertung von Röntgenbildern zur Erfassung von Parametern der Ellbogengelenksdysplasie. Teil 2: Stufenbildung im Gelenk Kleintierpraxis 1999;44:637–646

4. Viehmann B, Waibl H, Brunnberg L: Computergestützte Auswertung von Röntgenbildern zur Erfassung von Parametern der Ellbogengelenksdysplasie. Teil 1: Incisura trochlearis ulnae Kleintierpraxis 1999;44:595–606
5. Collins KE, Cross AR, Lewis DD, et al: Comparison of the radius of curvature of the ulnar trochlear notch of Rottweilers and Greyhounds. Am J Vet Res 2001;62:968-973
6. Gielen I, Van Ryssen B, Buijts J, et al: Canine elbow incongruity evaluated with computerized tomography (CT), radiography and arthroscopy Vet Radiol Ultrasound 2001:359
7. Preston CA, Schulz KS, Taylor KT, et al: In vitro experimental study of the effect of radial shortening and ulnar ostectomy on contact patterns in the elbow joint of dogs. Am J Vet Res 2001;62:1548-1556
8. Mason DR, Schulz KS, Samii VF, et al: Sensitivity of radiographic evaluation of radio-ulnar incongruence in the dog in vitro. Vet Surg 2002;31:125-132
9. Sjöström L, Kasström H, Kallberg M: Ununited anconeal process in the dog. Pathogenesis and treatment by osteotomy of the ulna. Vet Comp Orthop Traumatol 1995;8:170–176
10. Morgan JP, Wind A: Osteochondroses, hip dysplasia, elbow dysplasia., in Hereditary bone and joint diseases in the dog, Vol. Hannover, Germany, Schlütersche GmbH & Co., 1999, pp 41–94.
11. Van Ryssen B, van Bree H: Arthroscopic findings in 100 dogs with elbow lameness. Vet Rec 1997;140:360-362
12. Blond L, Dupuis J, Beauregard G, et al: Sensitivity and specificity of radiographic detection of canine elbow incongruence in an in vitro model. Vet Radiol Ultrasound 2005;46:210-216
13. Danielson KC, Fitzpatrick N, Muir P, et al: Histomorphometry of fragmented medial coronoid process in dogs: a comparison of affected and normal coronoid processes. Vet Surg 2006;35:501-509
14. Gemmill TJ, Clements DN: Fragmented coronoid process in the dog: is there a role for incongruency? J Small Anim Pract 2007;48:361-368
15. Samoy Y, Van Ryssen B, Gielen I, et al: Review of the literature: elbow incongruity in the dog. Vet Comp Orthop Traumatol 2006;19:1-8

16. Kramer A, Holsworth IG, Wisner ER, et al: Computed tomographic evaluation of canine radioulnar incongruence in vivo. *Vet Surg* 2006;35:24-29
17. Meyer-Lindenberg A, Fehr M, Nolte I: Co-existence of ununited anconeal process and fragmented medial coronoid process of the ulna in the dog. *J Small Anim Pract* 2006;47:61-65
18. Lozier SM: How I treat elbows in the older canine patient and new prospectives in elbow dysplasia Proceedings, Proceedings of the 13th European Society of Veterinary Orthopaedics and Traumatology (ESVOT) Congress, Munich, Germany, Sep 7th-10th, 2006
19. Wagner K, Griffon DJ, Thomas MW, et al: Radiographic, computed tomographic, and arthroscopic evaluation of experimental radio-ulnar incongruence in the dog. *Vet Surg* 2007;36:691-698
20. Werner H, Winkels P, Grevel V, et al: Sensitivity and specificity of arthroscopic estimation of positive and negative radio-ulnar incongruence in dogs. An in vitro study. *Vet Comp Orthop Traumatol* 2009;22:437-441
21. Böttcher P, Werner H, Ludewig E, et al: Visual estimation of radioulnar incongruence in dogs using three-dimensional image rendering: an in vitro study based on computed tomographic imaging. *Vet Surg* 2009;38:161-168
22. Taubin G: Estimation of planar curves, surfaces and nonplanar space curves defined by implicit equations, with applications to edge and range image segmentation. *IEEE Trans PAMI* 1991;13:1115-1138
23. Glas AS, Lijmer JG, Prins MH, et al: The diagnostic odds ratio: a single indicator of test performance. *J Clin Epidemiol* 2003;56:1129-1135
24. Holsworth IG, Wisner ER, Scherrer WE, et al: Accuracy of Computerized Tomographic Evaluation of Canine Radio-Ulnar Incongruence In Vitro. *Vet Surg* 2005;34:108-113
25. House MR, Marino DJ, Lesser ML: Effect of limb position on elbow congruity with CT evaluation. *Vet Surg* 2009;38:154-160

2.2 Relationship between axial radio-ulnar incongruence with cartilage damage in dogs with medial coronoid disease

Hamdi Eljack, BVM and Peter Böttcher, DVM, Prof. Dr. med. vet., Diplomate ECVS

Veterinary Surgery 2015; 44(2): 174-179.

Objective: To quantify axial radio-ulnar incongruence (aRUI) in dogs with simple fragmented medial coronoid process (FCP) and those with advanced medial coronoid disease (MCD).

Study Design: Retrospective clinical study

Sample Population: Group1: 54 elbow joints of 54 dogs with FCP, but no other visible cartilage damage. Group2: 32 elbows of 32 dogs with Outerbridge Grade 3 to 4 cartilage pathology at the medial coronoid \pm FCP.

Methods: aRUI was quantified using CT based 3D models of the radio-ulnar joint cup. A sphere was fitted to the trochlear notch of each of the 3D models and aRUI estimated in millimeters based on the relation of the sphere and the radial joint surface. Coronoid disease was diagnosed, classified and graded using arthroscopy.

Results: Mean aRUI for group1 was 0.2 mm (SD: 0.8), being significantly less ($P = 0.001$) than in group2 (mean aRUI = 0.8 mm [SD: 0.9]). Overall, 14% had negative aRUI, while 40% were congruent. Stepwise logistic regression analysis identified age and aRUI, but not body weight as significant covariates. The corresponding odds ratios for advanced MCD were 1.6 for age and 6.4 for RUI, respectively.

Conclusion: Axial RUI is greater and more prevalent in elbows with severe cartilage disease, and consists most commonly of a short radius.

Clinical Relevance: The heterogeneous distribution in degree and type of aRUI (including congruent joints) precludes the establishment of an uniform corrective osteotomy protocol in dogs with MCD.

Introduction

The aetiopathogenesis of fragmented medial coronoid process (FCP) as well as the development of cartilage degeneration and eburnation at the medial joint compartment are still poorly understood. The term “Medial Coronoid Disease” (MCD) has

recently been introduced^{1,2} summarizing different pathologies of the medial coronoid, including medial coronoid sclerosis, coronoid microfracture, coronoid fragmentation or fissuring, and cartilage damage to the coronoid process.³ Medial compartment disease of the elbow is characterized by loss of joint cartilage at the medial coronoid process and the humeral trochlea with or without fissuring or fragmentation of the medial coronoid process.³⁻⁶ Repetitive mechanical overloading of the medial compartment is thought to induce fatigue micro damage of the subchondral bone⁴ and subsequent overt fragmentation of bone and destruction of overlying articular cartilage.^{7,8} Radio-ulnar incongruence (RUI), mainly in the form of positive radio-ulnar incongruence with the radius being shorter relative to the ulna, has been stressed as one potential causative factor of mechanical overload within the medial compartment.^{9,10} Therefore, precise diagnosis of RUI seems to be fundamental to the investigation of potential surgical procedures to resolve elbow joint incongruence in dogs with significant RUI.¹¹ While an ongoing debate exists in the veterinary literature what degree of RUI is causing clinical problems,^{5,12-15} severe RUI ($\geq 2\text{-}3 \text{ mm}$) might correlate with the severity of mechanical overload and concomitant degenerative joint disease.^{4,5,9,10}

Currently, the most precise modalities to diagnose and grade RUI have been reported to be CT and arthroscopy.^{7,16,17} However, CT in form of reformatted sagittal and dorsal reconstructions still lacks perfect specificity and arthroscopy is highly operator dependent. A sphere fitted to the trochlear notch of CT based 3D renderings of the radio-ulnar joint cup has been shown to be highly sensitive and specific in vitro, while being operator independent at the same time.¹⁸ Mean sensitivity and specificity for detecting any form of incongruent joint using the sphere fitting technique has been reported to be 0.94 and 0.89, respectively.¹⁸ Because RUI is evaluated based on the geometry of the ulnar trochlear notch and the radial head, the technique measures axial RUI (aRUI) based on the geometric relation of the base of the medial coronoid process and the radial head at the midsagittal plane.

Because reformatted CT images failed to show a significant relation between the presence and amount of RUI, respectively, and degree of cartilage pathology within the medial joint compartment in clinical cases,⁵ the current study aims at investigating this relation using 3D modeling in combination with the sphere fitting technique. In extension to all previous work which only considered positive RUI, the sphere fitting

technique also allows for the detection and quantification of negative RUI and therefore negative as well as positive aRUI were to be investigated in the current study. This would allow to verify the hypotheses of the "Angular Vector Model",¹⁹ which considers both negative and positive RUI as a cause of mechanical overload of the medial joint compartment. The "Angular-Vector Model" is a theoretical extension of the "Traditional Linear Model",²⁰ in the way that both a short ulna (negative RUI) or short radius (positive RUI) lead to mechanical overloading of the medial compartment particularly the medial coronoid process and the humeral trochlea. The biomechanical concept for the short radius (positive RUI) is identical to the one of the "Traditional Linear Model"; however, with the "Angular-Vector Model" relative overgrowth of the radius (negative RUI; short ulna) is believed to increase intraarticular pressure within the medial joint compartment by pushing against the lateral aspect of the humeral condyle. Because the humeral condyle is in contact with the anconeal process, any pressure from the radial head will result in a rotatory moment with the anconeal process as pivot point, rotating the medial aspect of the humeral condyle distally, and therefore increasing the pressure at the medial coronoid process.¹⁹ Neither in-vitro nor clinical data are reported in peer reviewed literature which support this hypothesis.

Our working hypothesis was twofold: (1) positive aRUI would be associated with advanced medial coronoid disease and (2) a significant number of elbows ($\geq 15\ %$) with MCD will have negative aRUI.

Materials and Methods

Case Selection

Medical records (June 2006 – March 2011) were retrospectively reviewed to identify dogs admitted for elbow lameness. Dogs were eligible for inclusion when the diagnosis of medial coronoid disease had been confirmed using arthroscopy. In case both elbow joints were affected only one joint was included randomly using coin tossing. Including only one elbow in bilaterally affected cases was thought to increase the biological variance of the data.

Data extracted from medical records included breed, age and bodyweight (BW). Type and degree of MCD were based on arthroscopic images and videos. De-

pending on the entity of medial coronoid pathology two groups of dogs were defined: group 1 (g-FCP) were those elbow joints which had only a FCP without any other visible cartilage damage. Group 2 (g-MCD) were those joint which showed Outerbridge 3 to 4 cartilage damage at the medial coronoid process with or without concomitant FCP.

CT Image Acquisition

A complete transverse CT scan of both elbow joints was performed in dorsal recumbency with the elbow joint at an angle of ~135°, using a multi-slice helical CT-scanner (Philips Brilliance, Philips, Netherlands) with an average in-plane resolution of 0.4181 mm (SD = 0.0845 mm) and a slice thickness of 1 mm with an overlapping increment of 0.5 mm. Image reconstruction was done using a sharp bone filter (FilterType and ConvolutionKernel D).

Arthroscopy

After CT scanning, dogs in both groups had standard medial arthroscopic assessment of one or both elbow joints to confirm and document the type and degree of medial coronoid disease using a 30° for oblique 1.9 mm arthroscope (Karl Storz, Tuttlingen, Germany).²¹ Depending on the lesion simple fragment removal, subtotal coronoid osteotomy, dynamic proximal ulnar osteotomy (DPUO) or sliding humeral osteotomy (SHO) were performed alone or in combination.

3D Modeling

In each transverse CT data set, the humerus was manually segmented and removed from the data using MeVisLab (MeVisLab 2.0, MeVis Medical Solutions AG, Bremen, Germany, www.mevislab.de). Finally, three dimensional (3D) surface-reconstructions of the radio-ulnar joint cup were calculated using dedicated image analysis software based on the VTK (VTK 3.0, Kitware, Inc., NY, USA, www.vtk.org). Further enhancement as well as inspection of the so gained 3D-models were performed using ParaView (ParaView 3.0, Kitware, Inc., Clifton Park, NY, USA, www.paraview.org).

Sphere Fitting Technique

As previously described,¹⁸ a sphere was fitted to the ulnar trochlea of each 3D model of the radio-ulnar joint cup and evaluated for joint (in)congruence by the same investigator (HE). The degree of aRUI present was quantified based on the relation of the sphere and the caudal radial joint surface (see fig. 1a-c). Congruence was characterized by a continuous contact between the sphere and the caudal radial head. Positive aRUI was characterized by a clear space between the sphere and the radial head, while negative aRUI was diagnosed when the sphere collided with the radial head. By up- and down-scaling of the sphere's radius at 0.1 mm increments until the sphere touched the caudal radial joint surface like it would in a congruent joint, quantification of aRUI ranging from ≤ -3 to $\geq +3$ mm was performed.

Data Analysis

Statistical calculations were performed using software (SPSS 13.0 for Windows, SPSS Inc., Chicago, IL). Descriptive statistics for BW, age and aRUI were based on mean and standard deviation because of normal distribution of data, confirmed using the Kolmogorov-Smirnov test. Group comparison of g-FCP and g-MCD for BW, age and aRUI was done using unpaired t-test. Correlation of BW, age and aRUI within each group was assessed using Pearson correlation. A step-wise binary logistic regression model to predict the type of pathology (p-FCP vs. g-MCD) was developed, including BW, age and aRUI as covariates on first step. For all tests P was set to $\leq .05$.

Results

Eighty-six elbow joints met the inclusion criteria. Based on the arthroscopic findings 54 were assigned to g-FCP (21 left and 33 right) and 32 to g-MCD (15 left and 17 right). With a mean age of 3.1 years (SD: 2.6) in g-FCP and 4.6 years (SD: 3.5) in g-MCD, the latter were significantly older ($P = 0.04$), in average by 1.5 years (95% CI: 0.2 to 2.8). The mean body weight was 34.5 kg (SD: 8.6) and 34.6 kg (SD: 8.1), in g-FCP and g-MCD, respectively. In both groups male dogs were overrepresented, accounting for 70.4% and 68.8% in g-FCP and g-MCD, respectively. The most common breeds in g-FCP and g-MCD, respectively were as follows: Labrador Retriever

(18.5% and 12.5%), Golden Retriever (13.0% and 21.9%), Mixed-breed dog (18.5% and 12.5%), Bernese Mountain Dog (9.3% and 6.3%), Rottweiler (11.1 and 6.3%), and German Shepherd (7.5 and 8.4%).

Mean aRUI for g-FCP was 0.2 mm (SD: 0.8) and 0.8 mm (SD: 0.9) for g-MCD. Elbows in g-MCD tend to have a significantly larger aRUI ($P = 0.001$), in average by 0.7 mm (95% CI: 0.3 to 1.1). Rounding aRUI to the nearest integer value resulted in a frequency of aRUI in g-FCP with 1.9% ($n = 1$) having a -2 mm, 16.7% ($n = 9$) a -1 mm, 29.6% ($n = 16$) a +1 mm, 3.7% ($n = 2$) a +2 mm and 1.9% ($n = 1$) a +3 mm aRUI, while 46.3% ($n = 25$) were congruent. In g-MCD 3.1% ($n = 1$) had a -2 mm, 3.1% ($n = 1$) a -1 mm, 31.3% ($n = 10$) a +1 mm, and 34.4% ($n = 11$) a +2 mm aRUI with 28.1% ($n = 9$) being congruent (see fig. 2).

Weak correlations were found for bodyweight with age in g-FCP ($r = 0.341$, $P = 0.012$) and age with aRUI in g-FCP ($r = -0.270$, $P = 0.048$). The only strong correlation was found for age with aRUI in g-MCD ($r = -0.781$, $P = 0.000$) (see fig. 3).

The stepwise logistic regression model excluded BW as a significant covariate, leaving only age and aRUI in the equation. The corresponding odds ratios for having advanced MCD are summarized in table 1. The Hosmer–Lemeshow statistic for the model was 5.32 ($P = 0.72$) with 80.2 % of the cases being correctly classified.

Table 1: Odds Ratios of the significant Predictors for the Presence of Advanced Medial Coronoid Disease (group g-MCD) versus a Fragmented Medial Coronoid Process without other visible Cartilage Pathologies (group g-FCP) in a Logistic Regression Model

Predictor	Odds Ratio	
	(95% CI)	P-Value
Age (years)	1.563 (1.239 – 1.972)*	<.0005
RUI (millimeters)	6.362 (2.557 – 15.826) [#]	<.0005

* For each year of age, the animal is 1.563 times more likely to have Advanced Medial Coronoid Disease instead of an FCP without other visible cartilage damage

For each millimeter of positive RUI, the animal is 6.362 times more likely to have Advanced Medial Coronoid Disease instead of an FCP without other visible cartilage damage

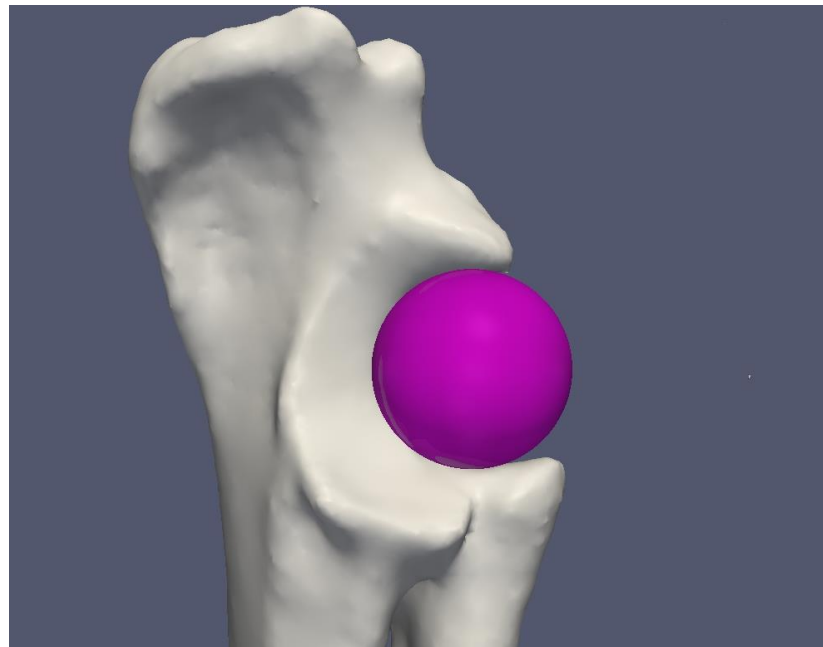


Fig 1a: 3D models of the radio-ulnar joint cup in combination with a sphere fitted to the trochlear notch of three different dogs. Congruence was characterized by a continuous contact between the sphere and the caudal radial head. Positive radio-ulnar incongruence (RUI) was characterized by a clear space between the sphere and the radial head, while negative RUI was diagnosed when the sphere collided with the radial head. (a) congruent radio-ulnar transition, (b) negative RUI of 2 mm, (c) positive RUI of 2 mm

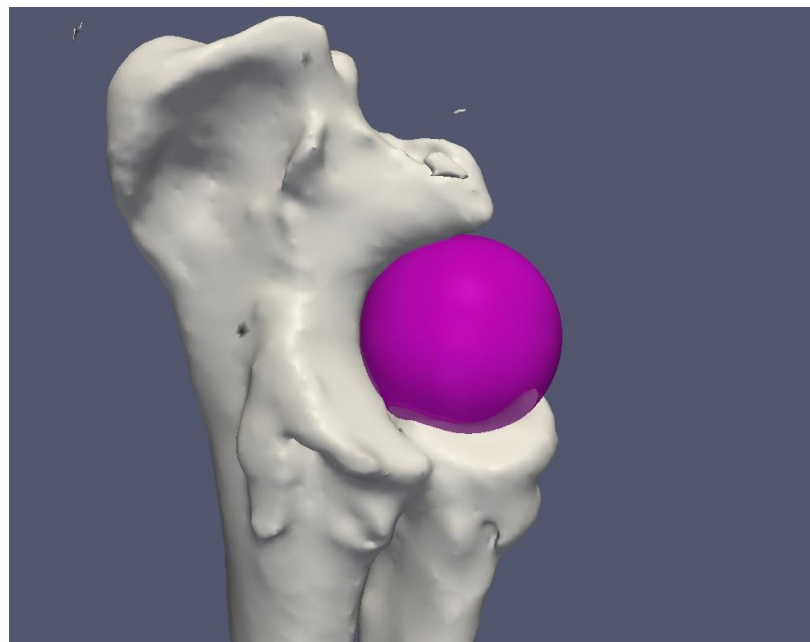


Fig 1b: 3D models of the radio-ulnar joint cup in combination with a sphere fitted to the trochlear notch of three different dogs. Congruence was characterized by a continuous contact between the sphere and the caudal radial head. Positive radio-ulnar incongruence (RUI) was characterized by a clear space between the sphere and the radial head, while negative RUI was diagnosed when the sphere collided with the radial head. (a) congruent radio-ulnar transition, (b) negative RUI of 2 mm, (c) positive RUI of 2 mm

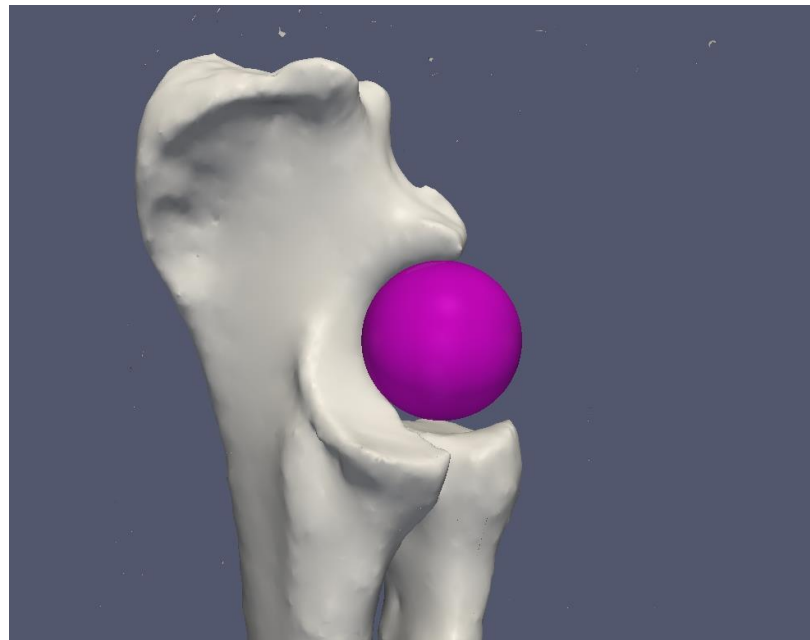


Fig 1c: 3D models of the radio-ulnar joint cup in combination with a sphere fitted to the trochlear notch of three different dogs. Congruence was characterized by a continuous contact between the sphere and the caudal radial head. Positive radio-ulnar incongruence (RUI) was characterized by a clear space between the sphere and the radial head, while negative RUI was diagnosed when the sphere collided with the radial head. (a) congruent radio-ulnar transition, (b) negative RUI of 2 mm, (c) positive RUI of 2 mm

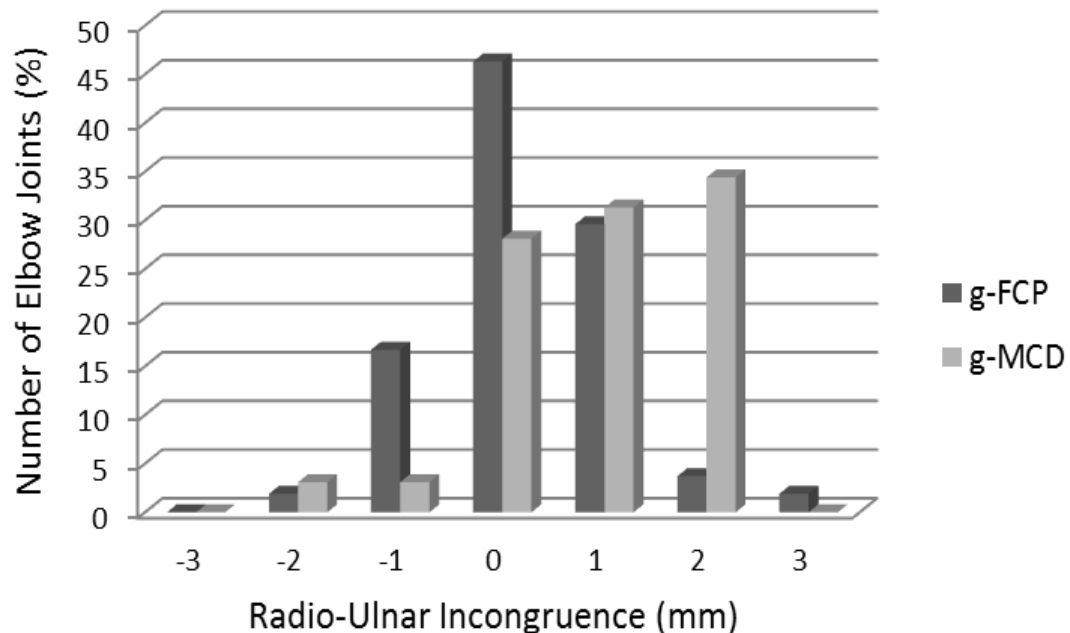


Fig 2: Prevalence and degree of radio-ulnar incongruence (RUI) in g-FCP ($n = 54$) and g-MCD ($n = 32$). Note the increasing frequency of large RUI in g-MCD and overall low prevalence of negative RUI in both groups.

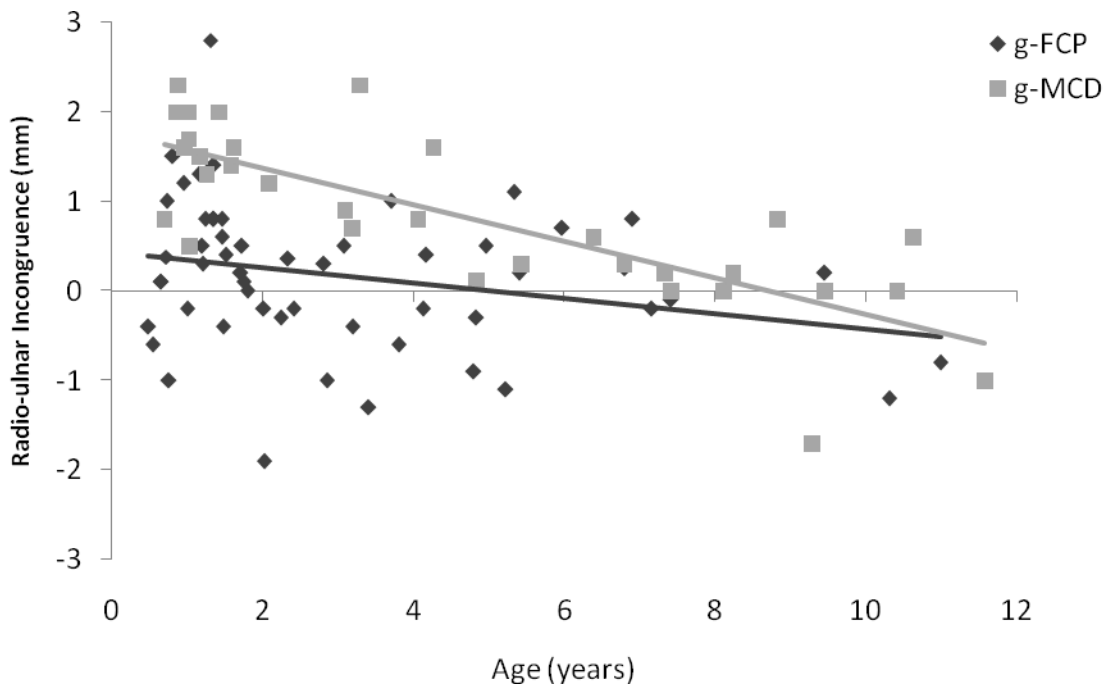


Fig 3: Pearson correlation of age and radio-ulnar incongruence (RUI) in g-FCP ($n = 54$; $r = -0.270$, $P = 0.048$) and g-MCD ($n = 32$; $r = -0.781$, $P = 0.000$).

Discussion

The present study shows a strong relationship between aRUI and the presence of advanced MCD, supporting the widely accepted hypothesis that RUI is one important aetiopathogenic factor in the development of medial coronoid disease.⁸⁻¹⁰ But the fact that altogether 40% of the investigated elbows appeared to be congruent (46 % in g-FCP and 28 % in g-MCD) suggests that other factors than incongruence alone may be involved. This is in agreement with previous studies, in which a significant number of elbows with MCD were free of detectable RUI.^{5,22} Therefore we propose to look at RUI as a secondary cause of MCD, potentially intensifying the detrimental effect of primary factors in the development of MCD. One of these primary factors might be joint instability.²³ Further studies investigating instability and aRUI in the same joints are needed to verify this hypothesis. The current study identified age as another significant covariate for advanced MCD. For each year the risk of having advanced MCD compared to simple FCP increases 1.6 times. RUI on the other hand impacts by factor 6.4 for each millimeter of aRUI. However these odds ratios cannot be interpreted independently, as both parameters were retained in the logistic regression model. With a mean difference in age of 1.5 years the dogs with advanced

MCD were significantly older than the dogs in g-FCP. That means that the dogs in g-MCD were in average 3.1 times more likely to have advanced MCD with the same amount of RUI, just because they tend to be slightly older. Nevertheless, with an odds ratio of 6.4, aRUI still remains the more important risk factor than age in the present study. The fact that dogs with large aRUI tend to present earlier in life in g-MCD was an unexpected finding. This probably reflects the clinical significance of aRUI in the development of advanced MCD, because dogs with large aRUI are more prone to develop advanced MCD and therefore will show clinical signs earlier in life than those with small aRUI.

We defined $\geq 15\%$ prevalence of aRUI to be of clinical significance, because this value matches the diagnostic threshold of CT,¹⁶ being the clinical gold standard for the detection of RUI. The relatively low prevalence of 14% for negative aRUI in the current study might render negative RUI, as an important pathomechanism of MCD, clinically insignificant. On the other hand, it supports the assumption of the Angular Vector Model, speculating that both positive and negative aRUI are involved in MCD. But as with every study investigating RUI with the dogs in dorsal recumbency and non-physiological joint load, the true state of joint (in)congruence during daily activity might be different to what we measured. Because most of the dogs which had negative aRUI belong to g-FCP, being significantly younger than those in g-MCD, laxity of the interosseous membrane might have allowed some axial positioning artifacts of radius and ulna relative to each other, resulting in false findings. Nevertheless, with a mean age of 3.1 years in g-FCP compared to 4.6 years in g-MCD, significant difference in the laxity of the interosseous membrane is considered very unlikely.

Overall, negative aRUI should probably not be regarded as a risk factor for the subsequent development of advanced MCD, as elbows with advanced pathologies, belonging to g-MCD, had negative aRUI only in two out of 32 joints (6%). On the other hand this is the first study to show that still a significant percentage (19%) of elbows with simple FCP had negative aRUI, something which has only been reported for ununited anconeal process with concomitant FCP so far.²⁴ Whether DPUO should be advised in these cases warrants further studies. Speculations, that the dogs in g-MCD are the same dogs than in g-FCP, but diagnosed at a later point in time when the disease has developed to a more advanced stage, raise the question what happened to the elbows with negative aRUI. One explanation would be that

negative RUI improved, becoming a congruent or even a joint with positive aRUI by time. This could only be answered when conducting longitudinal studies with follow-up CT. Because dogs in both groups had reached maturity (mean age in g-FCP 3.1 years vs. 4.6 years in g-MCD) adjustment of aRUI due to compensatory growth is unlikely. The only explanation for the difference in prevalence of negative aRUI between g-FCP and g-MCD would be that both groups represent different dogs with different disease. This would support our previous interpretation that negative aRUI is not a risk factor for advanced MCD.

Measuring RUI using radiographic technique is limited to the bony geometry of the joint. Arthroscopic evaluation, which has been shown to be highly accurate in vitro,^{16,17} would allow for the diagnosis of RUI at the level of the joint surface, even though arthroscopic assessment of RUI in a diseased joint with cartilage pathologies and bony fragments might not be as reliable than in vitro, and this is the main reason why quantification of RUI is not part of our arthroscopic protocol. Therefore RUI was not documented consistently in the arthroscopic reports of the dogs included in the current study, precluding any comparison between the arthroscopic and CT-based 3D-measurement of aRUI in this retrospective study. Griffon et al. showed that radiography, CT and arthroscopy did not correlate in respect to the degree of incongruence. Arthroscopy identified 21/36 joints as incongruent while radiography and CT only scored 7/27 and 13/37 as incongruent.⁶ In this special report incongruence on arthroscopy was mainly diagnosed at the apex of the medial coronoid process, while radiography and CT focused on the base of the coronoid process while evaluating RUI. This difference in localization raises an important aspect when comparing different imaging modalities and studies on RUI. The sphere fitting technique basically focuses on the relation of the sphere and the caudal radial head at the midsagittal plane, which might account for differences in prevalence of aRUI in the current report to previous studies. It should be emphasized that the sphere fitting technique has been validated¹⁸ using normal cadaveric elbow joints with an experimentally induced axial radio-ulnar step of known dimension, identical to previous validation studies investigating arthroscopy and CT.^{19,20} Nevertheless, it was not the aim of the current study to compare different modalities used for the quantification of positive aRUI, neither to compare our findings to previous once in an absolute way. Moreover, we compared aRUI in dogs with different degree of MCD rather than to compare aRUI in

dogs with normal joints and those with MCD. The fact that the sphere fitting technique has not yet been validated in respect to submillimeter precision is a limitation of the current study.

The sphere fitting technique has been shown to be a significant improvement over the purely subjective evaluation of RUI on 3D renderings of the radio-ulnar joint cup alone. Nevertheless, because aRUI is evaluated based on the geometry of the ulnar trochlear notch and the radial head, assessment of aRUI is based on the geometric relation of the base of the medial coronoid process and the radial head at the mid-sagittal plane. This is different to RUI at the apex of the coronoid process. Since RUI was not evaluated at the apex of the coronoid process, the possibility that the observed cartilage damage may be due to abnormalities other than aRUI cannot be eliminated. A small aRUI might be associated with an abnormal shape of the medial coronoid process or significant RUI at the apex.

Another bias in measuring aRUI in the current study could be attributed to the way the sphere is calculated. Because the sphere is fitted to the trochlear notch mismatch of the sphere and the radial head might not only be attributed to aRUI but also to trochlear notch dysplasia, which is one reported type of elbow incongruence.²⁰ Nevertheless, we consider significant bias from trochlear malformation unlikely as it is an uncommon condition, except for some breeds, such as Bernese Mountain dogs.²⁰

As already mentioned earlier positioning artifacts, inducing RUI artificially cannot be ruled out completely.²⁵ Adhering to a standardized scanning and positioning protocol was thought to limit such artifacts. At least analysis of inter group differences as well as correlation analysis should not be affected by such bias, as it would be the same for all elbow joints investigated. However, absolute values of RUI provided by studies using different modalities and different protocols to quantify RUI should be interpreted with caution.

Our findings suggest that already small aRUI may be involved in the development of advanced MCD, because elbows in group2 had a mean aRUI of 0.8 mm compared to the dogs with simple FCP (mean RUI = 0.2 mm). On the other hand a previous study proposed that RUI up to 2 mm might be physiological,¹⁶ an important detail which could not be verified, because we failed to include control elbows in the current study. RUI in normal joints would raise the question whether aRUI less than 2 mm

should be considered for surgical correction. Surgical treatment of medial coronoid disease differs greatly between surgeons. There is no broadly accepted treatment algorithm,²⁶ even though fragment removal and lavage or subtotal coronoid osteotomy either by open or arthroscopic approach are common procedures and might be regarded standard care.⁶ However, additional procedures such as DPUO, radial lengthening or ulnar shortening, SHO or proximal abducting ulnar osteotomy are debatable. Conzemius documented improvement in functional outcome following DPUO in only 10% of the cases when compared to fragment removal alone,²⁷ while Krotscheck et al. failed at documenting a significant improvement in humero-ulnoradial joint fit using proximal ulnar osteotomy with IM pin in cases with FCP without RUI.²⁸ However, a recent study with elbows having aRUI ≥ 2 mm demonstrated that DPUO ameliorates joint incongruence and focal joint contact at the medial coronoid. Evaluating each individual elbow for the presence and type of aRUI and performing DPUO selectively in those cases with proven RUI might yield better results than when using DPUO unselectively.

We conclude that positive axial RUI is more prevalent in elbows with advanced medial coronoid disease, while negative aRUI was only identified in 6% of elbows with advanced disease. However, with a prevalence of 19% in cases with simple FCP, negative aRUI might be of clinical importance in this group of patients. Overall, the heterogeneous distribution in degree and type of aRUI, including 40% congruent joints, precludes the establishment of a uniform corrective osteotomy protocol in dogs with MCD.

Bibliography

1. Fitzpatrick N, Smith TJ, Evans RB, et al: Subtotal coronoid osteotomy for treatment of medial coronoid disease in 263 dogs. Vet Surg 38:233-245, 2009.
2. Fitzpatrick N, Smith TJ, Evans RB, et al: Radiographic and arthroscopic findings in the elbow joints of 263 dogs with medial coronoid disease. Vet Surg 38:213-223, 2009.
3. Michelsen J: Canine elbow dysplasia. Aetiopathogenesis and current treatment recommendations. Vet J 196:12-19, 2013.
4. Danielson KC, Fitzpatrick N, Muir P, et al: Histomorphometry of fragmented medial coronoid process in dogs: a comparison of affected and normal coronoid

- processes. *Vet Surg* 35:501-509, 2006.
5. Kramer A, Holsworth IG, Wisner ER, et al: Computed tomographic evaluation of canine radioulnar incongruence in vivo. *Vet Surg* 35:24-29, 2006.
 6. Griffon D: Surgical diseases of the elbow, in Tobias KM, Johnston SA (eds): *Veterinary Surgery: Small Animal Vol.* St. Louis, Elsevier, 2012, pp 724-759.
 7. Boulay JP: Fragmented medial coronoid process of the ulna in the dog. *Vet Clin North Am Small Anim Pract* 28:51-74, 1998.
 8. Kirberger RM, Fourie SL: Elbow dysplasia in the dog: pathophysiology, diagnosis and control. *J S Afr Vet Assoc* 69:43-54, 1998.
 9. Gemmill TJ, Clements DN: Fragmented coronoid process in the dog: is there a role for incongruency? *J Small Anim Pract* 48:361-368, 2007.
 10. Samoy Y, Van Ryssen B, Gielen I, et al: Review of the literature: elbow incongruity in the dog. *Vet Comp Orthop Traumatol* 19:1-8, 2006.
 11. Holsworth IG, Wisner ER, Scherrer WE, et al: Accuracy of computerized tomographic evaluation of canine radio-ulnar incongruence in vitro. *Vet Surg* 34:108-113, 2005.
 12. Böttcher P, Werner H, Ludewig E, et al: Visual estimation of radioulnar incongruence in dogs using three-dimensional image rendering: an in vitro study based on computed tomographic imaging. *Vet Surg* 38:161-168, 2009.
 13. Samoy Y, Gielen I, Saunders J, et al: Sensitivity and specificity of radiography for detection of elbow incongruity in clinical patients. *Vet Radiol Ultrasound* 53:236-244, 2012.
 14. Samoy Y, Gielen I, Van Caelenberg A, et al: Computed tomography findings in 32 joints affected with severe elbow incongruity and fragmented medial coronoid process. *Vet Surg* 41:486-494, 2012.
 15. Samoy Y, Van Vynck D, Gielen I, et al: Arthroscopic Findings in 32 Joints Affected by Severe Elbow Incongruity with Concomitant Fragmented Medial Coronoid Process. *Vet Surg*, 2012.
 16. Wagner K, Griffon DJ, Thomas MW, et al: Radiographic, computed tomographic, and arthroscopic evaluation of experimental radio-ulnar incongruence in the dog. *Vet Surg* 36:691-698, 2007.

17. Werner H, Winkels P, Grevel V, et al: Sensitivity and specificity of arthroscopic estimation of positive and negative radio-ulnar incongruence in dogs. An in vitro study. *Vet Comp Orthop Traumatol* 22:437-441, 2009.
18. Eljack H, Werner H, Böttcher P: Sensitivity and specificity of 3D models of the radio-ulnar joint cup in combination with a sphere fitted to the trochlear notch for the estimation of radio-ulnar incongruence in vitro. *Vet Surg* 42:365-370, 2013.
19. Lozier S: How I treat elbows in the older canine patient and new prospectives in elbow dysplasia., Proceedings, Proceedings of the 13th European Society of Veterinary Orthopaedics and Traumatology (ESVOT) Congress, Munich, Germany, 2006 (available from
20. Wind AP: Elbow incongruity and developmental elbow diseases in the dog: Part I. *J Am Anim Hosp Assoc* 22:712-724, 1986.
21. Beale BS, Hulse DA, Schulz KS, et al: Arthroscopically assisted surgery of the elbow joint, in *Small Animal Arthroscopy* (ed 1), Vol. Philadelphia, Pennsylvania, USA, Sounders, 2003, p 510.
22. Gemmill TJ, Mellor DJ, Clements DN, et al: Evaluation of elbow incongruency using reconstructed CT in dogs suffering fragmented coronoid process. *J Small Anim Pract* 46:327-333, 2005.
23. Schmidt T, Fischer M, Böttcher P: Fluoroscopic kinematography of the sound and dysplastic canine elbow, in 16th European Society of veterinary Orthopaedics and Traumatology (ESVOT) Congress, Vol. Bologna, Italy, 2012.
24. Meyer-Lindenberg A, Fehr M, Nolte I: Co-existence of ununited anconeal process and fragmented medial coronoid process of the ulna in the dog. *J Small Anim Pract* 47:61-65, 2006.
25. House MR, Marino DJ, Lesser ML: Effect of limb position on elbow congruity with CT evaluation. *Vet Surg* 38:154-160, 2009.
26. Fitzpatrick N, Yeadon R: Working algorithm for treatment decision making for developmental disease of the medial compartment of the elbow in dogs. *Vet Surg* 38:285-300, 2009.
27. Conzemius M: Comparative Data for Treatment of Canine Elbow Dysplasia, in South European veterinary conference (SEVC), Vol. Barcelona, Spain, 2012.

28. Krotscheck U, Böttcher P, Thompson MS, et al: Cubital subchondral joint space width and CT osteoabsorptiometry in dogs with and without fragmented medial coronoid process. Vet Surg:DOI: 10.1111/j.1532-1950X.2014.12121.x, 2014.

3 Diskussion

Studien, die sich sowohl mit einer positiven als auch negativen RUI befassen, sind selten (WERNER et al. 2009, BÖTTCHER et al. 2009), und somit ist ein Vergleich unserer Ergebnisse mit anderen Untersuchungen, welche ausschließlich positive RUI kennen, nur eingeschränkt möglich (MASON et al. 2002, BLOND et al. 2005, WAGNER et al. 2007, HOLSWORTH et al. 2005). Mit Ausnahme der Arthroskopie, ist die neu entwickelte Kugel-Technik allen radiologischen Methoden überlegen, und die inakzeptabel geringe Spezifität reformatierter CT-Bilder bzw. von 3D-Rekonstruktionen konnte auf 0,89 erhöht werden. Sogar die interobserver Reliabilität stieg mit der Kugel-Technik von 0,87 auf 0,99 an und macht dieses Verfahren somit zu einem sehr guten klinischen Diagnostikum.

Die Kugel-Technik beruht auf der Annahme, dass in einem kongruenten Ellbogen die kreisförmige Geometrie des Sagittalkammes der *Incisura trochlearis* perfekt in die Oberfläche des kaudalen Aspekts des Radiuskopfes übergeht. Dies ist ein konstantes Merkmal in 3D-Modellen ohne RUI, und entsprechende Abweichungen werden in der vorliegenden Arbeit als positive bzw. negative RUI bezeichnet. Andere mögliche Formen der RUI, wie z.B. eine Stufenbildung im Bereich der Spitze des *Processus coronoideus medialis ulnae* werden mit dieser Technik nicht als solche erkannt.

Durch den Zusammenhang von Kugel-Technik und Geometrie der ulnaren *Incisura trochlearis* könnte die Kugel-Technik durch eine dysplastische Incisur verfälscht werden. Insbesondere eine zu kleine *Incisura trochlearis* ist als eine eigenständige Form der ED beschrieben (WIND 1986). Die berechnete Kugel wäre deutlich kleiner und würde eine positive RUI vorspiegeln. Ob dieses Szenario eine relevante Einschränkung bei der Verwendung der Kugel-Technik in klinischen Fällen ist, kann zum jetzigen Zeitpunkt nicht beantwortet werden, da bei der *in vitro* Validierung nur Ellbogengelenke ohne dysplastische Incisuren zur Verfügung standen.

Bei der Verwendung von CT basierten 3D-Modellen, gibt es einige Aspekte, die bei der klinischen Anwendung der Technik beachtet werden müssen (BÖTTCHER et al. 2009). Zuallererst berücksichtigen CT basierte Messung der RUI nur eine RUI auf der Ebene des subchondralen Knochens, unabhängig davon, ob multiplanare Rekonstruktionen oder 3D-Modelle verwendet werden. Deshalb kann man nicht mit

absoluter Sicherheit ausschließen, dass eine subchondrale RUI durch unterschiedliche Dicken der darüberliegenden Gelenkknorpel ausgeglichen werden könnte. Umgekehrt könnte eine echte RUI auf der Ebene der Gelenkfläche möglicherweise auf der Ebene des subchondralen Knochens unerkannt bleiben.

Eine weitere Einschränkung bei der Verwendung von CT-basierten Messungen sind mögliche Positionierungsartefakte während des CT-Scans (HOUSE et al. 2009). Ähnlich verhält es sich beim Grad der Extension und Rotation des Ellenbogens bei der Arthroskopie (WAGNER et al. 2007) oder Projektionsartefakten während des konventionellen Röntgens (BLOND et al. 2005). Aus diesem Grund ist für jede Modalität die standardisierte Positionierung der Gliedmaße während der Datenerfassung obligatorisch, um entsprechende Artefakte, zumindest innerhalb einer Modalität, auf das Minimum zu reduzieren. Allerdings sollten bei der Kugel-Technik Positionierungsartefakte von geringerer Relevanz sein, als z.B. bei reformatierten CT-Scans, da an den 3D-Modellen die konsistente Identifikation anatomischer Landmarken möglich ist (HOUSE et al. 2009). Die Identifizierung der Oberflächenpunkte zur Berechnung der Kugel ist intuitiv und sehr viel zuverlässiger als entsprechende Messpunkte auf multiplanaren Rekonstruktionen. Allerdings ist die Komplexität der Bildverarbeitungsschritte, um ein hochwertiges 3D-Modell der radio-ulnaren Gelenkpfanne zu generieren, wahrscheinlich die wichtigste Einschränkung der beschriebenen Technik, vor allem wenn man an eine klinische Anwendung denkt.

Schon alleine die Berechnung des 3D-Modells der radio-ulnaren Gelenkpfanne benötigt ca. 30 Minuten (BÖTTCHER et al. 2009), da eine manuelle Segmentierung des Humerus und anschließende Extraktion aus dem Datensatz durchgeführt werden muss, um einen freien Blick auf die Gelenkpfanne zu ermöglichen. Die manuelle Auswahl der Oberflächenpunkte entlang des sagittalen Grat der *Incisura trochlearis*, die Übertragung von Koordinaten für die Berechnung der Kugel und schließlich die Projektion der Kugel auf die virtuelle Szene, erhöhen nochmals den Zeitaufwand, bis man zu dem Punkt gelangt, an dem der Kliniker eine Diagnose stellen kann. Beide Verarbeitungsschritte, Segmentierung und Einbau der Kugel, müssten automatisiert werden, um eine breite klinische Anwendung zu ermöglichen. Etablierte Algorithmen für die automatische Segmentation der Knochen scheitern im kaninchen Ellenbogengelenk, da die Knochen bei der 3D-Rekonstruktion miteinander

verschmelzen. „3D third-order sub-pixel edge-driven level-set“ Segmentierung wurde bereits erfolgreich von unserer Arbeitsgruppe für diese Aufgabenstellung umgesetzt, aber der Code ist noch in der Entwicklungsphase und daher nicht für die öffentliche Nutzung verfügbar.

Auf Grund der guten Testparameter der Kugel-Technik wurden im zweiten Teil der Arbeit Hunde mit „Medial Compartment Disease“ (MCD) gegenüber solchen mit einer simplen Fragmentierung des medialen Kronfortsatzes, hinsichtlich Form und Ausprägung der RUI untersucht. Wir fanden einen starken Zusammenhang zwischen einer RUI und dem Vorhandensein einer MCD. Somit können wir die Annahme stützen, dass eine RUI ein wichtiger ätiopathogenetischer Faktor in der Entwicklung degenerativer Gelenkschäden im medialen Kompartiment ist (KIRBERGER und FOURIE 1998, GEMMILL und CLEMENTS 2007, SAMOY et al. 2006). Aber die Tatsache, dass 40 % der untersuchten Ellenbogen kongruent erschienen deutet darauf hin, dass auch andere Faktoren als eine RUI an der Ausbildung entsprechender Gelenkschäden beteiligt sind. Einer dieser Faktoren könnte eine rotatorische Gelenkinstabilität sein (SCHMIDT et al. 2012), welche zu unphysiologischen Belastungen innerhalb des Gelenkes führt, ohne dass eine RUI vorliegt.

Unsere aktuelle Studie identifiziert das Alter als weiteren bedeutenden Faktor für eine MCD. Dies bedeutet, dass Tiere die im höheren Alter mit ED vorstellig werden, in der Regel mehr Arthrose und stärkere Gelenkschäden aufweisen, als Tiere im jungen Alter. Somit kann man vermuten, dass über die Zeit auch kleinere RUIs zu einer schleichenden Degeneration des medialen Gelenkabschnittes führen.

Die relativ niedrige Prävalenz negativer RUI (14 %) stellt die Bedeutung des „Angular Vector Model“ in Frage, da in der aktuellen Studie die große Mehrzahl inkongruenter Gelenke eine positive Stufe aufwiesen. Andererseits sollte man bedenken, dass knapp 20 % der Tiere mit einer simplen Fragmentation des Kronfortsatzes eine negative Stufe aufwiesen und somit standardisierte Osteotomien, die vornehmlich auf die Korrektur einer positiven RUI abziehen, nicht sinnvoll sein können.

Auf der anderen Seite ist dies die erste Studie die zeigt, dass ein erheblicher Prozentsatz der Ellbogengelenke mit FCP eine negative RUI aufwiesen. Ein

Umstand der bisher nur für Tiere mit IPA und begleitendem FCP beschrieben ist (MEYER-LINDENBERG et al. 2006).

Zusammenfassend stellen wir fest, dass auch eine geringe RUI zur Entwicklung einer MCD beitragen kann, wobei positive wie auch negative Stufen auftreten. Dennoch ist die RUI nicht der einzige Faktor in der Ätiopathogenese, ein Umstand der bei invasiven Therapieformen, wie z.B. Osteotomien, in Zukunft mehr Berücksichtigung finden sollte.

4 Zusammenfassung

Hamdi Eljack

Bestimmung der radio-ulnaren Inkongruenz bei Hunden mit Ellbogengelenksdysplasie anhand von 3D-Rekonstruktionen

Klinik für Kleintiere der Veterinärmedizinischen Fakultät der Universität Leipzig

Eingereicht im Juni 2015

(39 Seiten, 5 Abbildungen, 3 Tabellen, 28 Literaturangaben)

Schlüsselwörter: Ellbogengelenk – radio-ulnare Inkongruenz – dreidimensional rekonstruierte CT-Modelle - Hund

Zielstellung: Die klinische Bedeutung einer radio-ulnaren Inkongruenz (RUI) bei Hunden mit Ellbogengelenksdysplasie, sowie die präzise Bestimmung einer geringgradigen RUI sind umstrittene Fragestellungen in der Kleintierorthopädie. Ziel der vorliegenden Studien war es (1) die 3D-Technik zur Bestimmung einer RUI in ihrer Genauigkeit zu verbessern und (2) mit Hilfe dieser verbesserten Technik, die Beziehung zwischen Ausprägung und Grad einer vorliegenden RUI und dem Ausmaß an damit verbundenen Gelenkschäden im medialen Kompartiment des Ellbogengelenkes zu untersuchen.

Material und Methoden: In einer ersten Studie wurden 63 CT-basierte 3D-Modelle der radio-ulnaren Gelenkpfanne mit bekannter RUI (-2mm, -1 mm, 0 mm, +1 mm, +2 mm), unter Verwendung einer Kugel, welche genau der *Incisura trochlearis* jedes individuellen Modells angepasst war, bezüglich der vorhanden RUI untersucht. Diese Messungen erfolgten geblendet in zufälliger Reihenfolge der 63 Modelle und wurden hinsichtlich Spezifität und Sensitivität ausgewertet.

In der zweiten Studie wurden 86 Ellbogengelenke klinischer Patienten retrospektiv mit der neuen 3D-Kugel-Methode bezüglich ihrer RUI vermessen. Dieser Wert wurde in Beziehung mit dem in der Arthroskopie diagnostizierten Gelenkschaden im

medialen Kompartiment gesetzt (Korrelation nach Pearson und logistische Regression), wobei die Gelenke in zwei Gruppen unterteilt wurden; die mit geringen Veränderungen (FPC-Gruppe) und solche mit fortgeschrittenen Schäden (MCD-Gruppe).

Ergebnisse: Unter Verwendung der Kugel-Methode betrug die mediane Sensitivität eine RUI auf einen Millimeter genau zu bestimmen 0,94 wobei die mediane Spezifität bei 0,89 lag. Der intra-Class-Korrelationskoeffizient für die interobserver Übereinstimmung betrug 0,99. 14 % der Gelenke wiesen eine negative RUI auf, 40 % zeigten keine messbare RUI und 46 % wiesen eine positive RUI auf. Das Quotenverhältnis (odds ratio) für das Vorliegen fortgeschrittener Gelenkschäden betrug für jeden Millimeter RUI 6,4.

Schlussfolgerungen: Die Anwendung der Kugel-Methode verbessert die Diagnose der RUI deutlich. Der vermutete Zusammenhang zwischen RUI und Gelenkschäden konnte mit der klinischen Studie bestätigt werden. Allerdings ist bemerkenswert, dass 40 % der Gelenke keine RUI aufwiesen. Somit ist davon auszugehen, dass andere Faktoren neben einer RUI an der Pathogenese klinisch beobachteter Gelenkschäden beteiligt sind. Ebenso ist festzustellen, dass ca. 15 % der Gelenke eine negative RUI aufweisen. Somit scheint es nicht gerechtfertigt alle Gelenke mit einer Form der Ellbogenosteotomie zu behandeln, da eine negative bzw. positive RUI und insbesondere keine RUI unterschiedliche geometrische Korrekturen benötigen.

5 Summary

Hamdi Eljack

Estimation of radio-ulnar incongruence in dogs with elbow dysplasia based on 3D image rendering

Department of Small Animal Medicine, Faculty of Veterinary Medicine, University of Leipzig

Submitted in June 2015

(39 pages, 5. figures, 3 tables, 28 references)

Keywords: elbow joint – radioulnar incongruence– three-dimensional image rendering – dog

Objectives: The clinical significance of RUI in dogs with elbow dysplasia and precise estimation of small degree of RUI are controversial topics in small animal orthopedics. The aim of this study was to (1) improve the accuracy of the 3D technique for the estimation of RUI and (2) using the improved technique to examine the relationship between the shape and degree of present RUI and the amount of related joint damage in the medial compartment of the elbow joint.

Material and methods: In a first study, 63 CT-based 3D models of the radio-ulnar joint cup with known RUI (-2 mm, -1 mm, 0 mm, +1, +2 mm) were examined using a sphere, which was exactly fitted to the trochlear ulnar notch of each individual model. The assessment of the radioulnar joint conformation was evaluated blindly in a random manner and analyzed in respect to sensitivity and specificity. In the second study, 86 elbow joints of clinical patients were retrospectively graded with the new 3D sphere technique with respect to their RUI. This value was correlated with the arthroscopically diagnosed joint damage in the medial compartment, where the joints were divided into two groups. Those with minor changes (g-FPC) and those with advanced damage (g-MCD).

Results: By using the sphere fitting technique, the median sensitivity of a RUI on a millimeter basis was 0.94 and the median specificity was 0.89. The intra-class correlation coefficient for interobserver agreement was 0.99. In the clinical joints 14 % had a negative RUI, 40 % showed no measurable RUI and 46% had a positive RUI. The odds ratio for the presence of advanced joint damage for every millimeter RUI was 6.4

Conclusions: The application of the sphere fitting technique significantly improves the diagnosis of the RUI. The assumed relationship between RUI and joint damage could be confirmed in the clinical study. However, it is noteworthy that 40 % of the joints showed no RUI. Thus, it can be assumed that other factors besides RUI are playing rule in the pathogenesis of clinically observed joint damages.

Also it should be noted that approximately 15 % of the joints have a negative RUI. Thus, it does not seem to be wise to treat all the joints with a type of elbow osteotomy, as a negative or positive RUI and in particular no RUI need different geometric corrections

6 Literaturverzeichnis

- Blond L, Dupuis J, Beauregard G, Breton L, Moreau M. Sensitivity and specificity of radiographic detection of canine elbow incongruence in an in vitro model. *Vet Radiol Ultrasound.* 2005;46:210-6.
- Böttcher P, Brauer S, Werner H. Estimation of joint incongruence in dysplastic canine elbows before and after dynamic proximal ulnar osteotomy. *Vet Surg.* 2013;42:371-6
- Böttcher P, Werner H, Ludewig E, Grevel V, Oechtering G. Visual estimation of radioulnar incongruence in dogs using three-dimensional image rendering: an in vitro study based on computed tomographic imaging. *Vet Surg.* 2009;38:161-8.
- Brannberg L, Viehmann B, Waibl H. Computergestützte Auswertung von Röntgenbildern zur Erfassung von Parametern der Ellbogengelenksdysplasie; Teil 2: Stufe im Gelenk. *Kleintierpraxis.* 1999;44:637-46.
- Collins KE, Cross AR, et al. Comparison of the radius of curvature of the ulnar trochlear notch of Rottweilers and Greyhounds. *Am J Vet Res.* 2001;62:968-73.
- Conzemius M. Comparative Data for Treatment of Canine Elbow Dysplasia. South European veterinary conference (SEVC); 2012 Oct.18-20; Parcerala, Spain
- Danielson KC, Fitzpatrick N, Muir P, Manley PA. Histomorphometry of fragmented medial coronoid process in dogs: a comparison of affected and normal coronoid processes. *Vet Surg.* 2006;35:501-9.
- Gielen I, Van Rijssen B, Buijts J, Lückerath R, van Bree H. Canine Elbow Incongruity Evaluated With Computerised Tomography (CT), Radiography and Arthroscopy. *Vet Radiol Ultrasound.* 2001;42:359-94.
- Gemmill TJ, Clements DN. Fragmented coronoid process in the dog: is there a role for incongruency? *J Small Anim Pract.* 2007;48:361-8.
- Gemmill TJ, Mellor DJ, Clements DN, Clarke SP, Farrell M, Bennett D, Carmichael S. Evaluation of elbow incongruency using reconstructed CT in dogs suffering fragmented coronoid process. *J Small Anim Pract.* 2005;46:327-33.
- Gielen I, van Ryssen B, van Bree H. Arthrology-diagnostic imaging: is CT the answer? Proceedings of the 12th European Society of Veterinary Orthopaedics and Traumatology (ESVOT) Congress; 2004 Sep 10-12; Munich, Germany; p.140.

- Holsworth IG, Wisner ER, Scherrer WE, Filipowitz D, Kass PH, Pooya H, Larson RF, Schulz KS. Accuracy of computerized tomographic evaluation of canine radio-ulna incongruence in vitro. *Vet Surg.* 2005;34:108-13.
- House MR, Marino DJ, Lesser ML. Effect of limb position on elbow congruity with CT evaluation. *Vet Surg.* 2009;38:154-60.
- Kirberger RM, Fourie SL. Elbow dysplasia in the dog: pathophysiology, diagnosis and control. *J S Afr Vet Assoc.* 1998;69:43–54.
- Kramer A, Holsworth IG, Wisner ER, Kass PH, Schulz KS. Computed tomographic evaluation of canine radioulnar incongruence in vivo. *Vet Surg.* 2006;35:24-9.
- Krotscheck U, Bottcher PB, Thompson MS, Todhunter RJ, Mohammed HO. Cubital subchondral joint space width and CT osteoabsorptiometry in dogs with and without fragmented medial coronoid process. *Vet Surg.* 2014;43:330-8.
- Lozier SM. How I treat elbows in the older canine patient and new prospectives in elbow dysplasia. Proceedings of the 13th European Society of Veterinary Orthopaedics and Traumatology (ESVOT) Congress; 2006 Sep. 7-10; Munich, Germany; p.93-6.
- Mason DR, Schulz KS, Samii VF, Fujita Y, Hornof WJ, Herrgesell EJ, Long CD, Morgan JP, Kass PH. Sensitivity of radiographic evaluation of radio-ulnar incongruence in the dog in vitro. *Vet Surg.* 2002;31:125-32.
- Meyer-Lindenberg A, Fehr M, Nolte I. Co-existence of ununited anconeal process and fragmented medial coronoid process of the ulna in the dog. *J Small Anim Pract.* 2006;47:61-5.
- Morgan JP, Wind A, Davidson AP. Bone dysplasias in the Labrador Retriever: a radiographic study. *J Am Anim Hosp Assoc.* 1999;35:332-40.
- Preston CA, Schulz KS, Taylor KT, Kass PH, Hagan CE, Stover SM. In vitro experimental study of the effect of radial shortening and ulnar ostectomy on contact patterns in the elbow joint of dogs. *A J Vet Res.* 2001;62:1548-56.
- Schmidt T, Fischer M, Böttcher P. Fluoroscopic kinematography of the sound and dysplastic canine elbow. 16th European Society of veterinary Orthopaedics and Traumatology (ESVOT) Congress; 2012 Sep.12-15; Bologna, Italy.
- Samoy Y, Van Ryssen B, Gielen I, Walschot N, van Bree H. Review of the literature: elbow incongruity in the dog. *Vet Comp Orthop Traumatol.* 2006;19:1-8.

Sjostrom L, Kasstrom H, Kallberg M. Ununited anconeal process in the dog pathogenesis and treatment by osteotomy of the ulna. *Vet Comp Orthop Traumatol.* 1995;8:170-6.

Wagner K, Griffon DJ, Thomas MW, Schaeffer DJ, Schulz K, Samii VF, Necas A. Radiographic, computed tomographic, and arthroscopic evaluation of experimental radio-ulnar incongruence in the dog. *Vet Surg.* 2007;36:691-8.

Werner H, Winkels P, Grevel V, Oechtering G, Böttcher P. Sensitivity and specificity of arthroscopic estimation of positive and negative radio-ulnar incongruence in dogs. An in vitro study. *Vet Comp Orthop Traumatol.* 2009;22:437-41.

Wind AP. Elbow incongruity and developmental elbow diseases in the dog.1. *J Am Anim Hosp Assoc.* 1986;22:711-24.

Wind AP, Packard ME. Elbow incongruity and developmental elbow diseases in the dog.2. *J Am Anim Hosp Assoc.* 1986;22:725-30.

Danksagung

An erster Stelle möchte ich mich bei Herrn Prof. Dr. Gerhard Oechtering für die Möglichkeit der Anfertigung der Dissertation an der Klinik für Kleintiere der Universität Leipzig bedanken.

Zweitens möchte ich mich bei der Universität Khartum für die Erteilung eines Stipendiums, um die Anfertigung der Doktorarbeit in Deutschland bedanken.

Mein besonderer Dank geht an meinen Betreuer Herrn Prof. Dr. Peter Böttcher für die Überlassung des Themas, die ständige kompetente Betreuung, die wertvollen Ratschläge und die fortwährende Hilfsbereitschaft.

Ein weiterer großer Dank geht an die Mitarbeiterinnen und Mitarbeiter der Klinik für Kleintiere der Universität Leipzig, insbesondere an alle Mitarbeiter der chirurgischen Abteilung für die freundliche und angenehme Arbeitsatmosphäre.

Besonders herzlich danke ich meiner Familie, vor allem meinen Eltern und meiner Ehefrau Maysaa Dafalla. Ohne sie wäre all dies nicht möglich gewesen.

